Supplemental material

Disson et al., https://doi.org/10.1084/jem.20181210

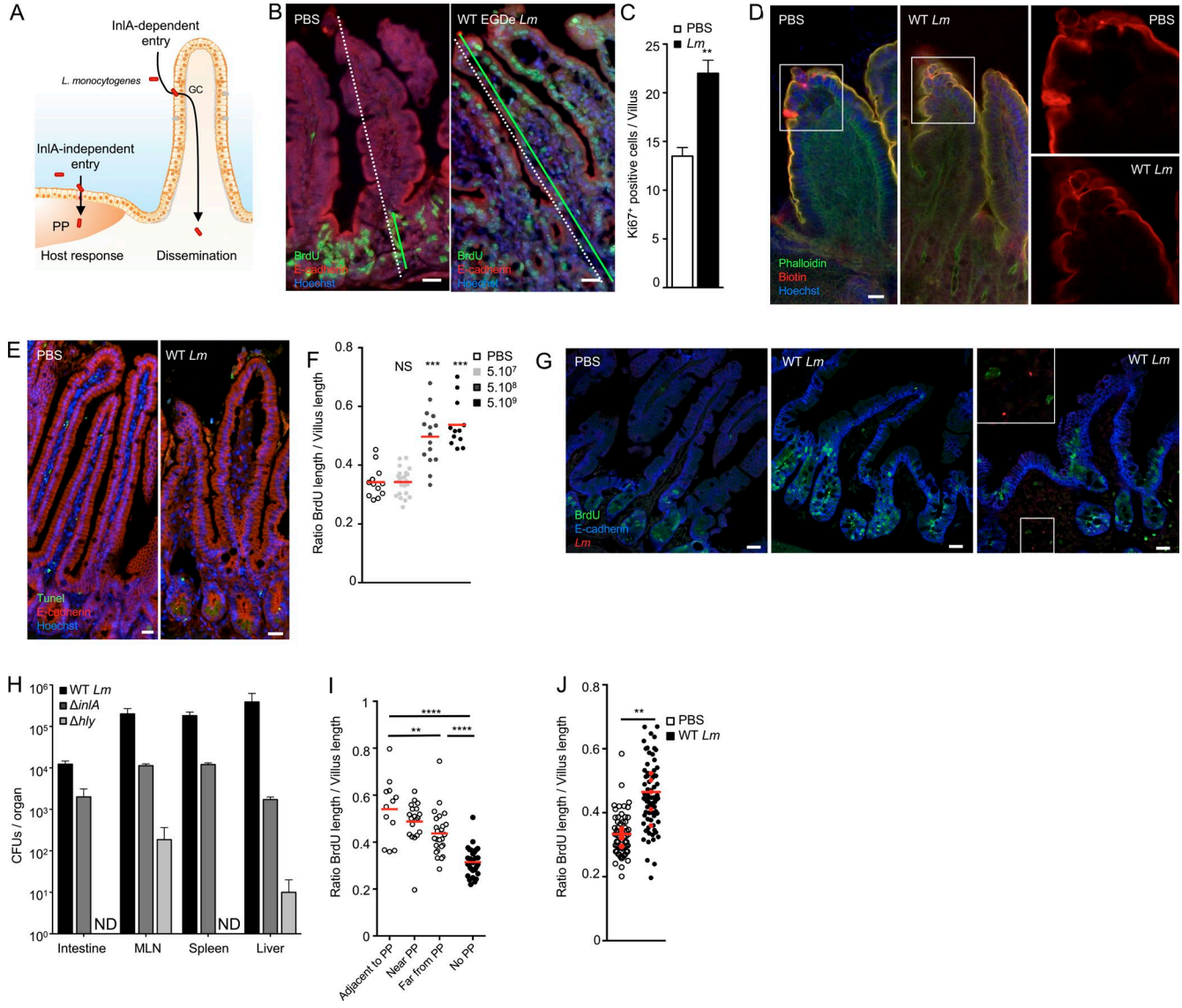

Figure S1. **Characterization of *Lm*-induced epithelial cell proliferation. (A)** *Lm* entry in InlA-dependent and -independent entry (Lecuit et al., 2007; Nikitas et al., 2011). **(B)** Fluorescent imaging of frozen sections of the ileum obtained from KIE16P mice 4 d after oral infection with 5 × 10^9 EGDe *Lm* strain. 16 h before euthanasia, mice were injected with BrdU. Sections are stained for proliferating cells (BrdU), epithelial cells (Ecad), and nuclei (Hoechst). Bars, 20 µm. **(C)** Quantification of KI67$^+$ cells in KIE16P mice 2 d after oral infection with 5 × 10^9 *Lm*. *n* = 4–8 villi. Data are represented as mean ± SEM. Mann-Whitney test. **(D)** Confocal imaging of frozen sections of the ileum obtained from KIE16P mice 3 d after oral infection with 5 × 10^9 *Lm*. Biotin was injected into ileum loop followed by PBS wash and fixation. Sections are stained for actin (phalloidin) and nuclei (Hoechst). Bars, 20 µm. **(E)** Confocal imaging of frozen sections of the ileum obtained from KIE16P mice 4 d after oral infection with 5 × 10^9 *Lm*. Dead cells are labeled by a TUNEL assay. Tissue is stained for epithelial cells (Ecad) and Nuclei (Hoechst). Bars, 20 µm. **(F)** Quantification of dose-dependent epithelial proliferation. Each dot corresponds to one quantified villus. Mann-Whitney test. **(G)** Confocal imaging of frozen sections of the ileum obtained from KIE16P mice 4 d after oral infection with 5 × 10^9 WT *Lm* strain. Sections are stained for BrdU, epithelial cells (Ecad), and WT *Lm*. Bars, 20 µm. **(H)** *Lm* burden in organs of KIE16P mice infected with 5 × 10^9 CFUs of WT *Lm* strain, Δ*inlA*, and Δ*hly* isogenic mutants 4 d after oral inoculation. Data are represented as mean ± SEM. ND, not detected. **(I)** Quantification of epithelial proliferation in ligated loop of KIE16P mice containing one or no PP infected with 10^5 Δ*inlA Lm* 24 h pi. Each dot corresponds to one quantified villus. Adjacent to PP are villi next to PPs. Near PP are the 10 villi next to adjacent villi. Far from PP are the other villi. Data are extracted from two mice per condition, representative of two independent experiments. A one-way ANOVA test followed by a Tukey's multiple comparisons was performed. **(J)** Quantification of epithelial proliferation in C57BL/6J mice infected with 5 × 10^9 *Lm*. Each dot corresponds to one quantified villus, except the red dots, which correspond to the mean of each mouse. *n* = 5 mice/strain. A Mann-Whitney test was performed. **, P < 0.01; ***, P < 0.001; ****, P < 0.0001.

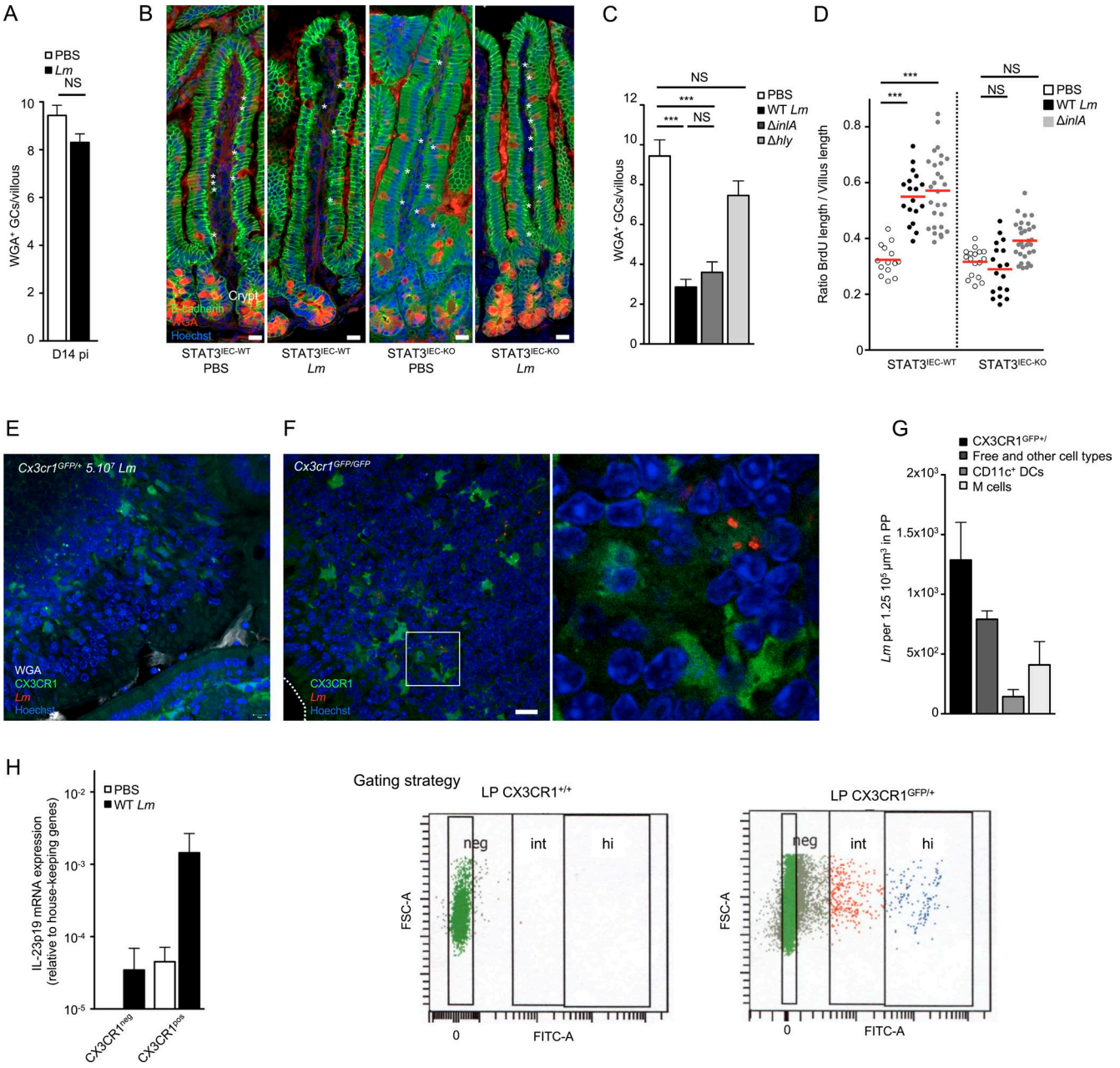

Figure S2. ***Lm*-associated epithelial cell proliferation and decrease of WGA⁺ GCs depend on STAT3 and CX3CR1. (A)** Quantification of WGA⁺ GCs/villous 14 d after inoculation. *n* = 30–33 villi/condition. Data are represented as mean ± SEM. Mann-Whitney test. **(B)** Confocal imaging of frozen sections of the ileum obtained from $STAT3^{IEC\text{-}WT}$ and $STAT3^{IEC\text{-}KO}$ mice 4 d after oral infection with 5 × 10^9 *Lm*. Sections are stained for mucus (WGA), epithelial cells (Ecad), and nuclei (Hoechst). Bars, 20 µm. **(C)** Quantification of WGA⁺ GCs/villous in KIE16P mice infected by WT EGD *Lm* and isogenic mutants 4 d after inoculation. *n* = 10–23 villi/condition. Data are representative of two independent experiments. Data are represented as mean ± SEM. Mann-Whitney test. **(D)** Quantification of epithelial proliferation in KIE16P $STAT3^{IEC\text{-}WT}$ and KIE16P $STAT3^{IEC\text{-}KO}$ mice infected by WT *Lm* or the isogenic mutant Δ*inlA*. Mann-Whitney test. Each dot corresponds to one quantified villus. *n* = 2 mice/strain. **(E)** Confocal imaging of a vibratome section from a PP infected by 5 × 10^7 *Lm* 24 h after oral inoculation. **(F)** Confocal imaging of a vibratome section from a $CX3CR1^{GFP/GFP}$ PP infected by 5 × 10^9 CFUs *Lm* 24 h after oral inoculation. Bar, 20 µm (E and F). **(G)** Quantification of *Lm* in PP cells from vibratome sections of $CX3CR1^{GFP/+}$ mice infected by 5 × 10^9 CFUs *Lm* 24 h after oral inoculation. Data are represented as mean ± SEM. **(H)** IL-23 mRNA quantification by qRT-PCR on sorted ileal (LP + PP) $CX3CR1^{-}$ and $CX3CR1^{+}$ cells 24 h pi. Data are representative of two independent experiments with at least three mice per group. Data are represented as mean ± SEM. ***, P < 0.001.

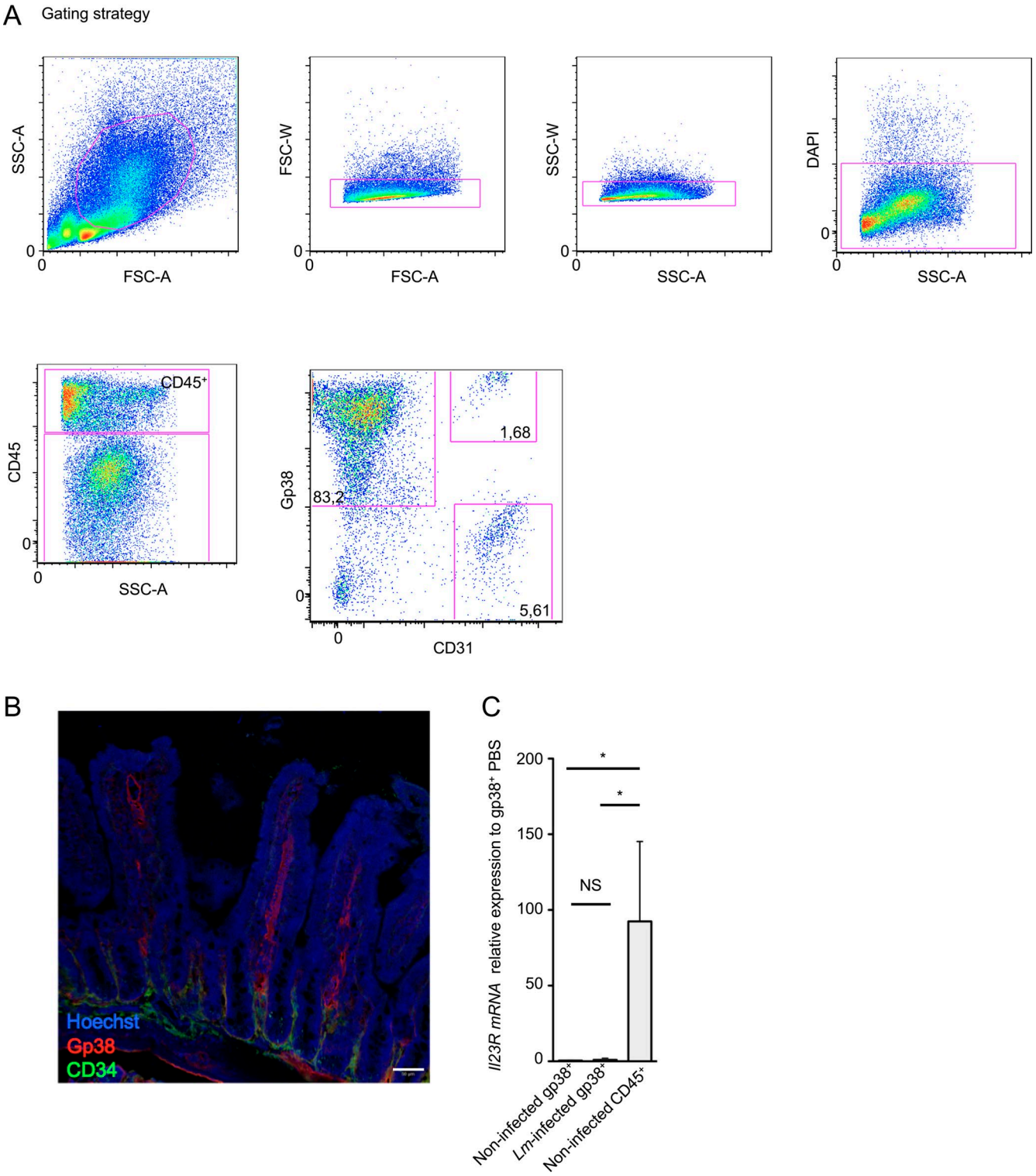

Figure S3. **Characterization of gp38⁺ stromal cells expressing *Il11*. (A)** Gating strategy to define the CD45⁺, CD45⁻CD31⁻gp38⁺ and CD31⁺ cells. Numbers in flow plots indicate the percentage of cells in the gate. **(B)** Confocal imaging of frozen sections of the ileum. Section is stained for gp38 (red), CD34 (green), and Hoechst (blue). Bar, 50 µm. **(C)** *Il23R* mRNA quantification by qRT-PCR from ileal LP sorted CD45⁺ and CD45⁻ gp38⁺ stromal cells 48 h pi. Data are represented as mean ± SEM. A one-way ANOVA test followed by a Sidak's multiple comparisons was performed. *, P < 0.05.

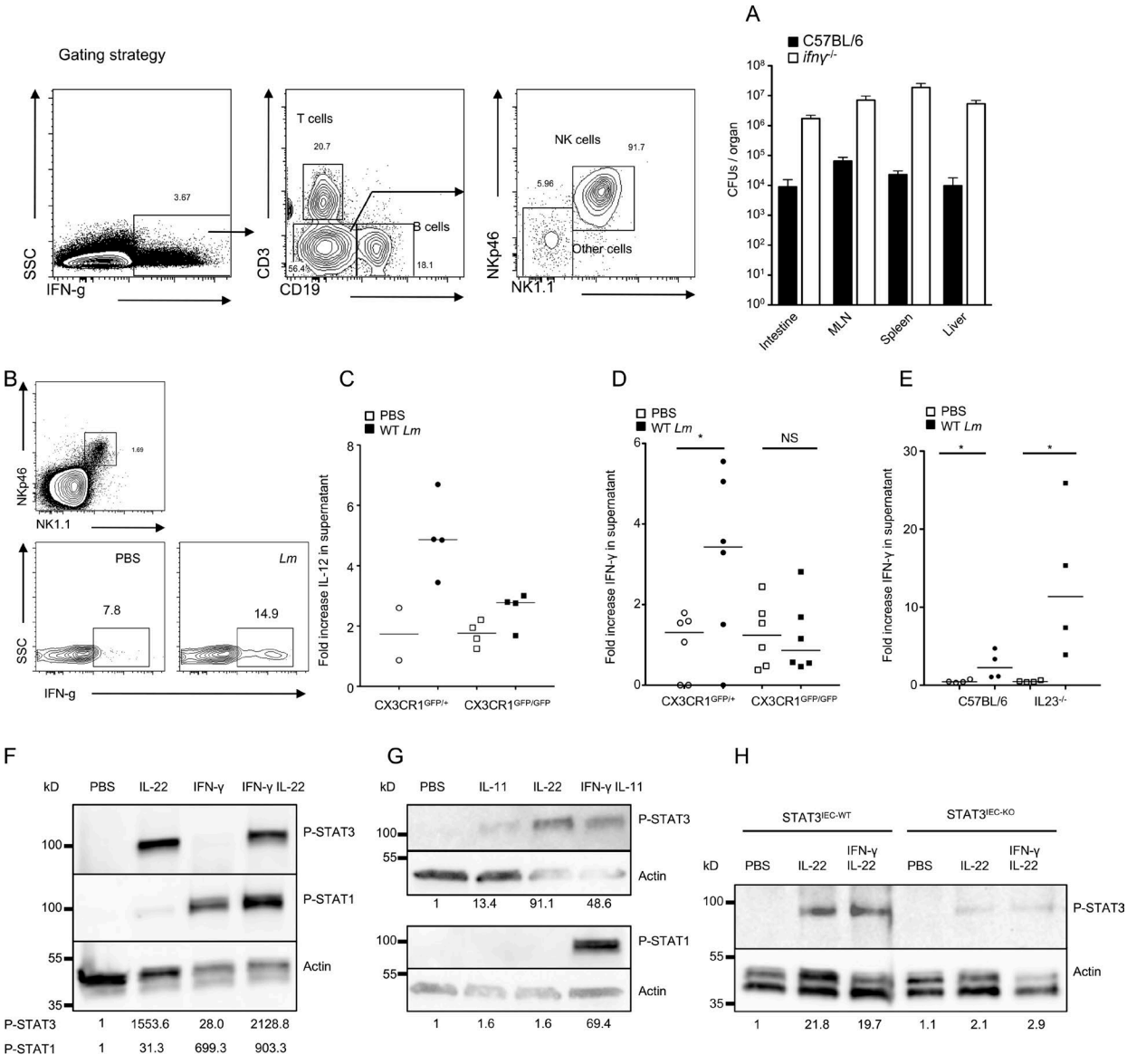
A
Gating strategy
SSC
IFN-g
3.67
CD3
CD19
T cells
20.7
B cells
56.4
18.1
NKp46
NK1.1
NK cells
91.7
5.96
Other cells
C57BL/6
ifnγ-/-
CFUs / organ
Intestine
MLN
Spleen
Liver
B
NKp46
NK1.1
1.69
PBS
Lm
7.8
14.9
SSC
IFN-g
C
PBS
WT Lm
Fold increase IL-12 in supernatant
CX3CR1GFP/+
CX3CR1GFP/GFP
D
PBS
WT Lm
*
NS
Fold increase IFN-γ in supernatant
CX3CR1GFP/+
CX3CR1GFP/GFP
E
PBS
WT Lm
*
*
Fold increase IFN-γ in supernatant
C57BL/6
IL23-/-
F
kD
PBS
IL-22
IFN-γ
IFN-γ IL-22
P-STAT3
P-STAT1
Actin
100
100
55
35
P-STAT3 1 1553.6 28.0 2128.8
P-STAT1 1 31.3 699.3 903.3
G
kD
PBS
IL-11
IL-22
IFN-γ IL-11
P-STAT3
Actin
P-STAT1
Actin
100
55
100
55
1 13.4 91.1 48.6
1 1.6 1.6 69.4
H
STAT3IEC-WT
STAT3IEC-KO
kD
PBS
IL-22
IFN-γ IL-22
PBS
IL-22
IFN-γ IL-22
P-STAT3
Actin
100
55
35
1 21.8 19.7 1.1 2.1 2.9
I

Figure S4. **IFN-γ and IL-23 pathways are both involved in *Lm*-associated epithelial cell proliferation.** Gating strategy to define the B, T, and NK cells from ileal LP**.** Numbers in flow plots indicate the percentage of cells in the gate. **(A)** *Lm* burden in organs of C57BL/6 and *Ifnγ*$^{-/-}$ mice infected with 5 × 10^{9} CFUs of WT *Lm* 4 d after oral inoculation. Data are represented as mean ± SEM. **(B)** Example of IFN-γ quantification by flow cytometry analysis of NKp46^{+} NK1.1^{+} NK cells 2 d after oral infection. Numbers in flow plots indicate the percentage of cells in the gate. **(C)** IL-12 protein quantification by an ELISA assay from total ileal tissue of *Cx3cr1*$^{GFP/GFP}$ and *Cx3cr1*$^{GFP/+}$ 2 d after oral inoculation. Each dot corresponds to one mouse. Median is shown. **(D)** IFN-γ protein quantification by an ELISA assay from total ileal tissue of *Cx3cr1*$^{GFP/GFP}$ and *Cx3cr1*$^{GFP/+}$ 2 d after oral inoculation. Each dot corresponds to one mouse. Median is shown. Data are pooled from two independent experiments. Student's *t* test. **(E)** IFN-γ protein quantification by an ELISA assay from total ileal tissue of WT C57BL/6J and *IL23*$^{-/-}$ mice 2 d after oral inoculation. Each dot corresponds to one mouse. Median is shown. Student's *t* test. **(F)** Western blot analysis of STAT3 and STAT1 phosphorylation in organoids upon IL-22 and IFN-γ treatment. kD corresponds to the molecular weight of the band ladder. **(G)** Western blot analysis of STAT3 and STAT1 phosphorylation in organoids upon IL-11, IL-22, and IFN-γ treatment. **(H)** Western blot analysis of STAT3 phosphorylation in STAT3$^{IEC\text{-}WT}$ and in STAT3$^{IEC\text{-}KO}$ organoids upon IL-22 and IFN-γ treatment. Quantification has been done by dividing the intensity of the phosphorylated band by the intensity of the actin band, and normalized to the PBS treated control organoids. **(I)** ICY script to quantify areas from confocal acquired images. *, $P < 0.05$.

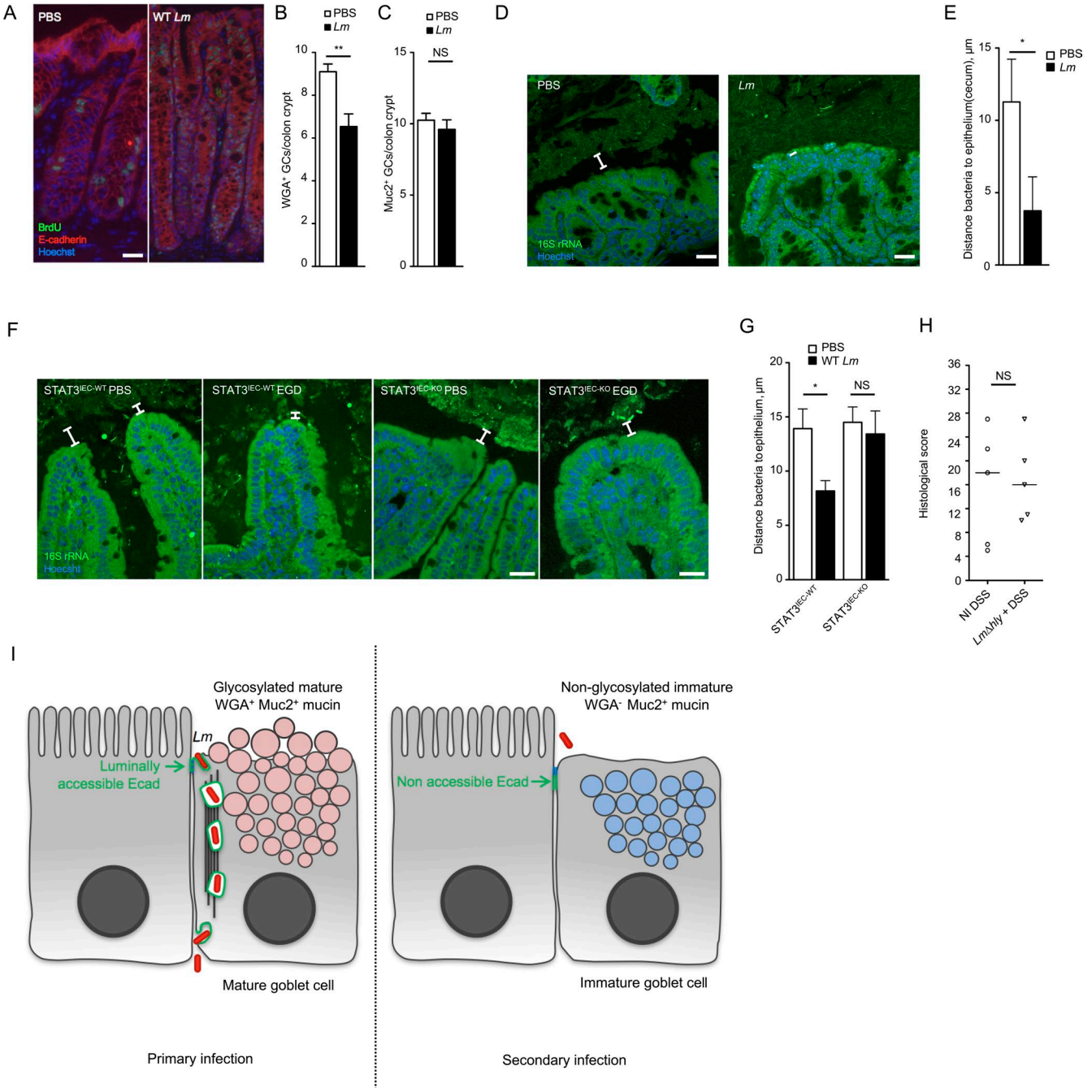

Figure S5. ***Lm*-associated decrease of WGA⁺ GCs is associated with mucus layer thinning. (A)** Fluorescent imaging of frozen sections of the colon obtained from KIE16P mice 4 d after oral infection with 5 × 10^9 EGD WT *Lm* strain. 16 h before euthanasia, mice were injected with BrdU. Sections are stained for proliferating cells (BrdU), epithelial cells (Ecad), and nuclei (Hoechst). Bars, 20 µm. **(B)** Quantification of WGA⁺ GCs per colon crypt 4 d after inoculation. *n* = 20–30 independent crypts. Data are represented as mean ± SEM. Mann-Whitney test. **(C)** Quantification of Muc2⁺ GCs per colon crypt 4 d after inoculation. *n* = 20–30 independent crypts. Data are represented as mean ± SEM. Mann-Whitney test. **(D)** Confocal imaging of sections of Carnoy's fixed cecum obtained 5 d pi with 5 × 10^9 *Lm*. Sections are stained for microbiota 16S rRNA and nuclei (Hoechst). Bars, 20 µm. **(E)** Quantification of distance between microbiota and the epithelium, in micrometers. *n* = 8 independent measures. Data are represented as mean ± SEM. Mann-Whitney test. **(F)** Confocal imaging of sections of Carnoy's fixed ileum obtained 5 d pi with 5 × 10^9 *Lm*. Sections are stained for microbiota 16S rRNA and nuclei (Hoechst). Bars, 20 µm. **(G)** Quantification of distance between microbiota and the epithelium, in micrometers. *n* = 12–24 independent villi. Data are represented as mean ± SEM. Mann-Whitney test. **(H)** Score of histological lesions induced in DSS-treated mice. DSS, DSS-treated mice; NI, not infected; Each dot represents one mouse. Median is shown. Student's *t* test. **(I)** Model of GC differentiation upon *Lm* infection. Left: Mature GCs express glycosylated mucin and accessible Ecad. Right: Upon *Lm* infection, GCs do not fully differentiate and do not express accessible Ecad. *, P < 0.05; **, P < 0.01.

References

Lecuit, M., J.L. Sonnenburg, P. Cossart, and J.I. Gordon. 2007. Functional genomic studies of the intestinal response to a foodborne enteropathogen in a humanized gnotobiotic mouse model. *J. Biol. Chem.* 282:15065–15072. https://doi.org/10.1074/jbc.M610926200

Nikitas, G., C. Deschamps, O. Disson, T. Niault, P. Cossart, and M. Lecuit. 2011. Transcytosis of Listeria monocytogenes across the intestinal barrier upon specific targeting of goblet cell accessible E-cadherin. *J. Exp. Med.* 208:2263–2277. https://doi.org/10.1084/jem.20110560